

Tunable cooperativity in a spin-crossover Hoffman-like metal-organic framework material by Aromatic Guests

Jin-Yan Li, Chun-Ting He, Yan-Cong Chen, Ze-Min Zhang, Wei Liu, Zhao-Ping Ni* and Ming-Liang Tong*

Key Laboratory of Bioinorganic and Synthetic Chemistry of Ministry of Education, School of Chemistry and Chemical Engineering, Sun Yat-Sen University, Guangzhou 510275, P. R. China

Experimental Section

All reagents are commercial and used without purification. Elemental analysis was carried on Elementar Vario-EL CHN elemental analyzer. Powder X-ray diffraction was performed on Bruker D8 Advance diffractometer at room temperature (the scanning range and rate were 4-50° and 0.2 °/s, respectively). The kinds and amounts of solvents were determined by Thermogravimetry coupled to a Mass Spectrometer, STA449 F3 Jupiter-QMS 403C aedo. FT-IR spectroscopy was carried out on Bio-Rad FTS-7 spectrometer at room temperature in the range of 4000-400 cm⁻¹. Magnetic data were collected on a Quantum Design PPMS instrument or Quantum Design SQUID magnetometer under a magnetic field of 1000 Oe with the sweeping rate of 2 K/min. Then the diamagnetic correction was operated from Pascal's constants, while the background of the sample holder was experimentally determined before.

X-ray diffraction: Single crystal X-ray diffraction data were collected on Agilent SuperNova CCD diffractometer with Cu_{Kα} radiation ($\lambda = 1.54178 \text{ \AA}$) at 95(2) K and 250(2) K, respectively. The structures were solved by direct methods, and all non-hydrogen atoms were refined anisotropically by least-squares on F^2 using the SHELXTL program. Hydrogen atoms on organic ligands were generated by the riding mode.¹ The disordered DMF, ethanol and cyclohexane molecules could not be modelled properly; thus, we used the program SQUEEZE,² a part of the PLATON package of crystallographic software, to calculate the solvent disorder area and move away their contributions to the overall intensity data.

1. G. M. Sheldrick, *SHELXTL97, program for crystal structure refinement*, University of Göttingen, Germany, 1997.
2. P. Van Der Sluis, A. L. Spek, *Acta Crystallogr. Sect. A*, 1990, **46**, 194.

Table S1. Crystallographic data for the as-synthesized complex.

<i>T</i> [K]	95(2)	250(2)
empirical formula	C _{26.3} H _{26.7} N _{7.5} O _{1.8} Au ₂ Fe	
formula weight	926.43	
crystal system	Monoclinic	
space group	<i>P</i> 2 ₁ / <i>m</i>	
<i>a</i> [Å]	10.1153(3)	10.4681(4)
<i>b</i> [Å]	10.0824(3)	10.4451(4)
<i>c</i> [Å]	15.4366(6)	15.8449(6)

$\beta / ^\circ$	100.790(4)	104.194(4)
$V [\text{\AA}^3]$	1546.49(9)	1679.60(11)
Z	2	
$D_c (\text{mg cm}^{-3})$	1.990	1.832
$F(000)$	871	871
$\mu(\text{Cu}_{K\alpha}) (\text{mm}^{-1})$	21.471	19.770
crystal size (mm)	0.15×0.11×0.03	0.15×0.11×0.03
No. of total reflections	3206	3466
No. of reflections [$I > 2\sigma(I)$]	2677	2861
$R_I[I > 2\sigma(I)]^a$	0.0533	0.0557
$wR[I > 2\sigma(I)]^a$	0.1534	0.1641
S	1.078	1.066

Table S2. Selected bond lengths [\AA] and angles [deg] for the as-synthesized complex.

	95 K	250 K
Fe(1)-N(1)	1.930(8)	2.182(8)
Fe(1)-N(2)	1.930(8)	2.133(8)
Fe(1)-N(3)	1.918(7)	2.125(7)
Fe(1)-N(3)^[a]	1.918(7)	2.125(7)
Fe(1)-N(4)	1.995(7)	2.229(7)
Fe(1)-N(5)^[b]	2.017(8)	2.233(7)
Au(1)-C(1)	1.993(9)	1.984(8)
Au(1)-C(2)^[c]	2.016(10)	1.997(9)
Au(2)-C(3)	1.962(10)	1.979(7)
Au(2)-C(3)^[d]	1.962(10)	1.979(7)
Au(1)⋯Au(2)^[e]	3.1097(5)	3.1413(5)
N(1)-Fe(1)-N(3)	90.91(17)	91.41(15)
N(1)-Fe(1)-N(3)^[a]	90.91(17)	91.41(15)
N(1)-Fe(1)-N(2)	179.7(3)	178.9(3)
N(1)-Fe(1)-N(4)	91.4(3)	90.5(3)
N(1)-Fe(1)-N(5)^[b]	86.8(3)	85.4(3)
N(2)-Fe(1)-N(3)	89.09(17)	88.58(15)
N(2)-Fe(1)-N(3)^[a]	89.09(17)	88.58(15)
N(2)-Fe(1)-N(4)	88.8(3)	88.5(3)
N(2)-Fe(1)-N(5)^[b]	92.9(3)	95.7(3)
N(3)-Fe(1)-N(3)^[a]	177.7(3)	177.1(3)
N(3)-Fe(1)-N(4)	89.31(16)	89.66(14)
N(3)^[a]-Fe(1)-N(4)	89.31(16)	89.66(14)
N(3)-Fe(1)-N(5)^[b]	90.72(16)	90.44(14)
N(3)^[a]-Fe(1)-N(5)^[b]	90.72(16)	90.44(14)
N(4)-Fe(1)-N(5)^[b]	178.2(3)	175.8(3)

C(1)-Au(1)-C(2)^[c]	178.0(4)	178.0(3)
C(3)-Au(2)-C(3)^[d]	177.3(4)	176.3(4)

Symmetry codes: a) $x, -y+1/2, z$; b) $x, y, z+1$; c) $x-1, y, z$; d) $x, -y+3/2, z$; e) $-x+1, -y+1, -z+1$.

Table S3. The numbers of guests for different clathrates were determined by TG analysis.

Clathrate	1 ·C ₆ H ₁₂	1 ·CS ₂	1 ·Benzene	1 ·Naphthalene	1 ·Anthracene	1 ·Ferrocene
Guest number	1.5	1.4	0.9	0.7	0.3	0.4

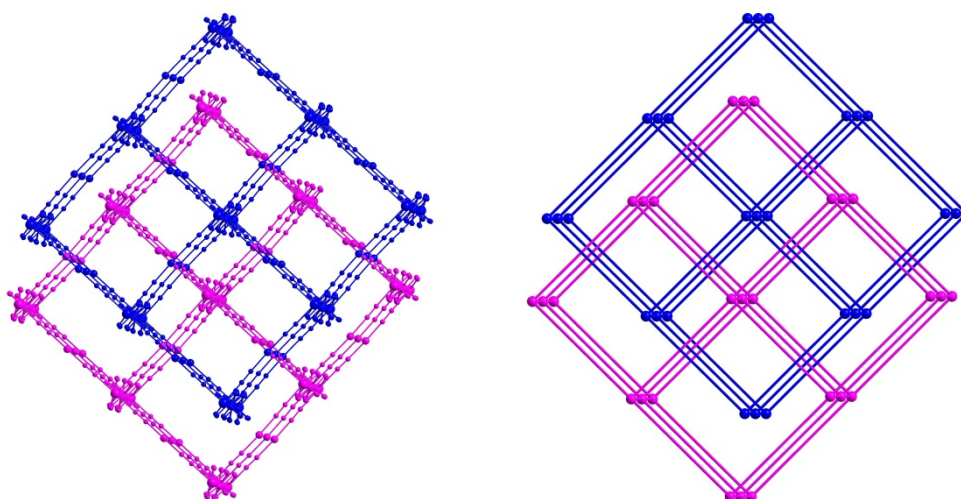


Figure S1. The 3D interpenetrated framework of as-synthesized complex (left), and its corresponding topological network (right). The Schläfli symbol for this uninodal net is described as $(4^{12}.6^3)$, corresponding to the prototypical pcu net.

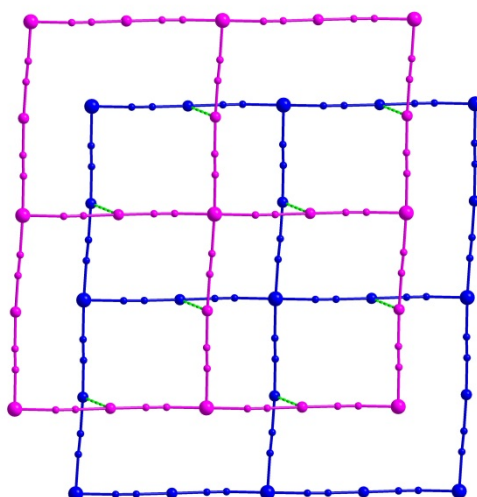


Figure S2. The aurophilic interactions between two closest $[\text{Fe}\{\text{Au}(\text{CN})_2\}_2]_\infty$ layers.

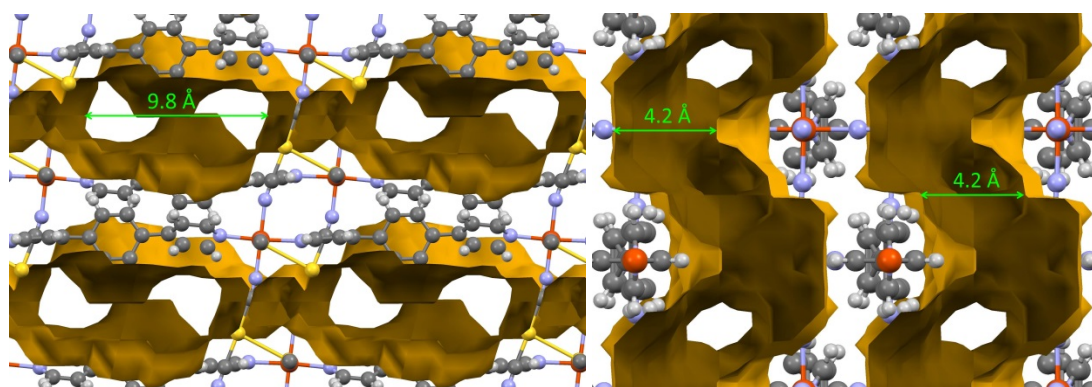


Figure S3. Views of 1D channel along *b* axis (left) and its cross section from *c* axis (right).

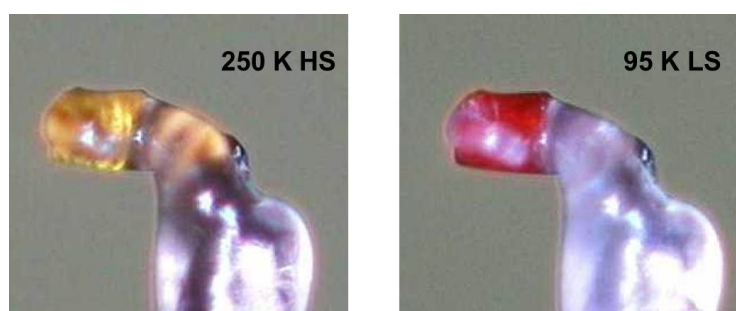


Figure S4. Thermochromism of the as-synthesized complex.

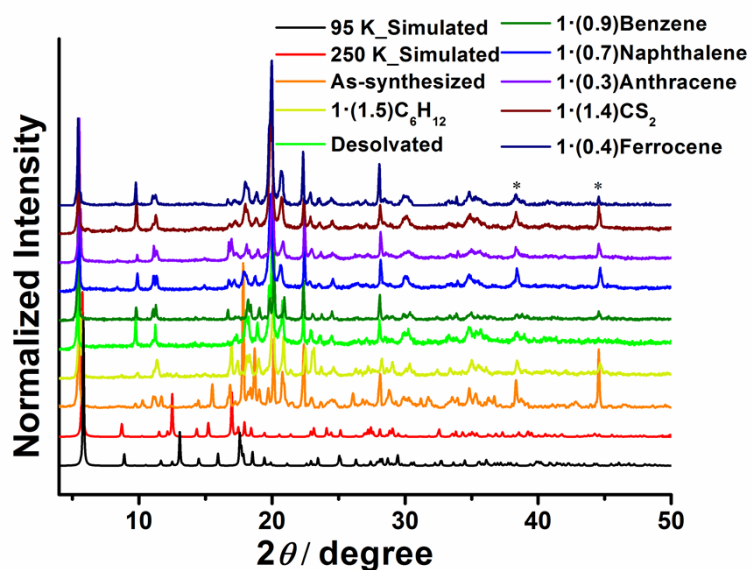


Figure S5. Powder X-ray diffraction patterns of different samples and simulated forms. The peaks marked with * were due to silicon carrier.

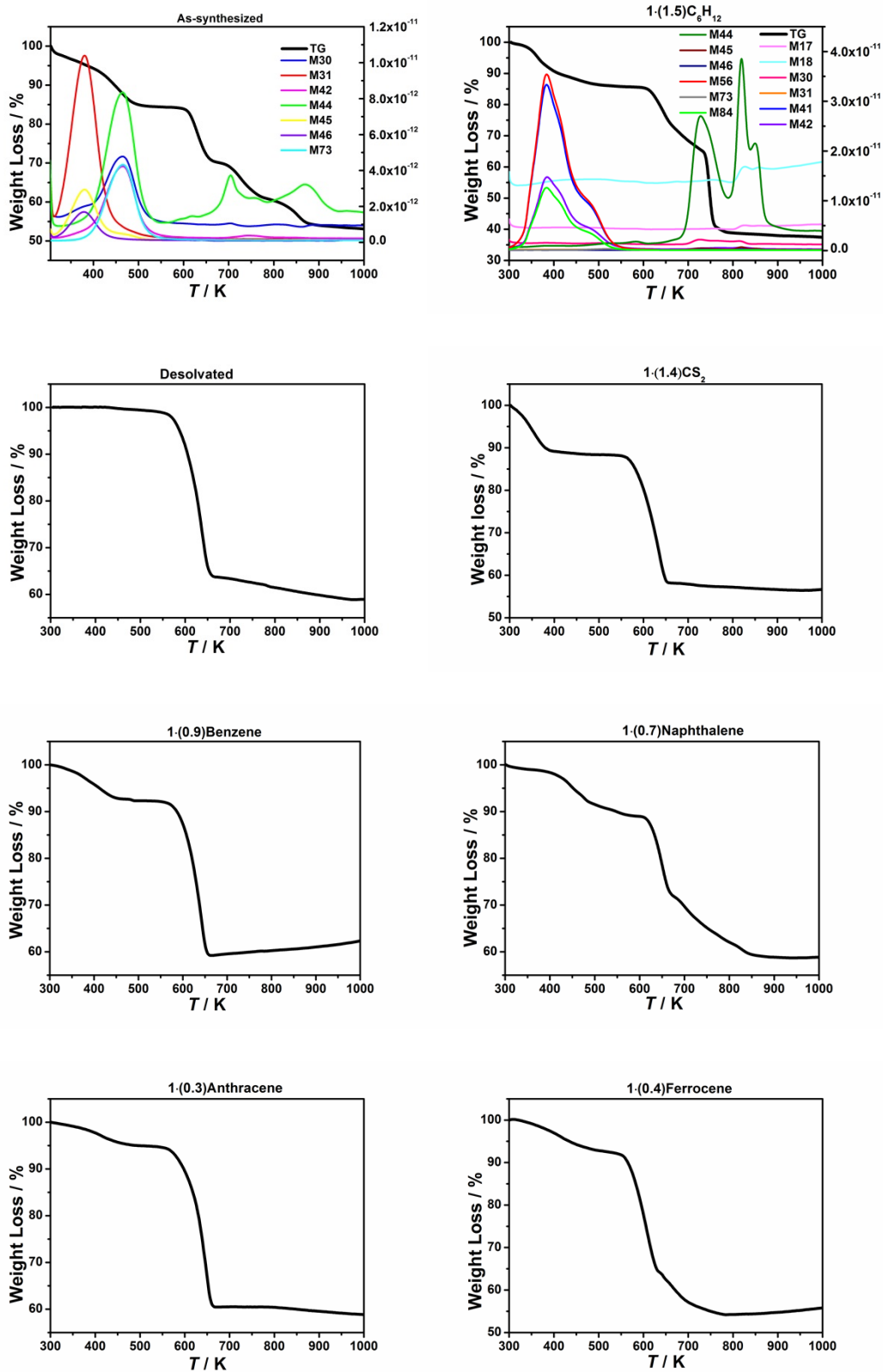


Figure S6. Thermogravimetric or thermogravimetric-mass spectra analysis of various complexes.

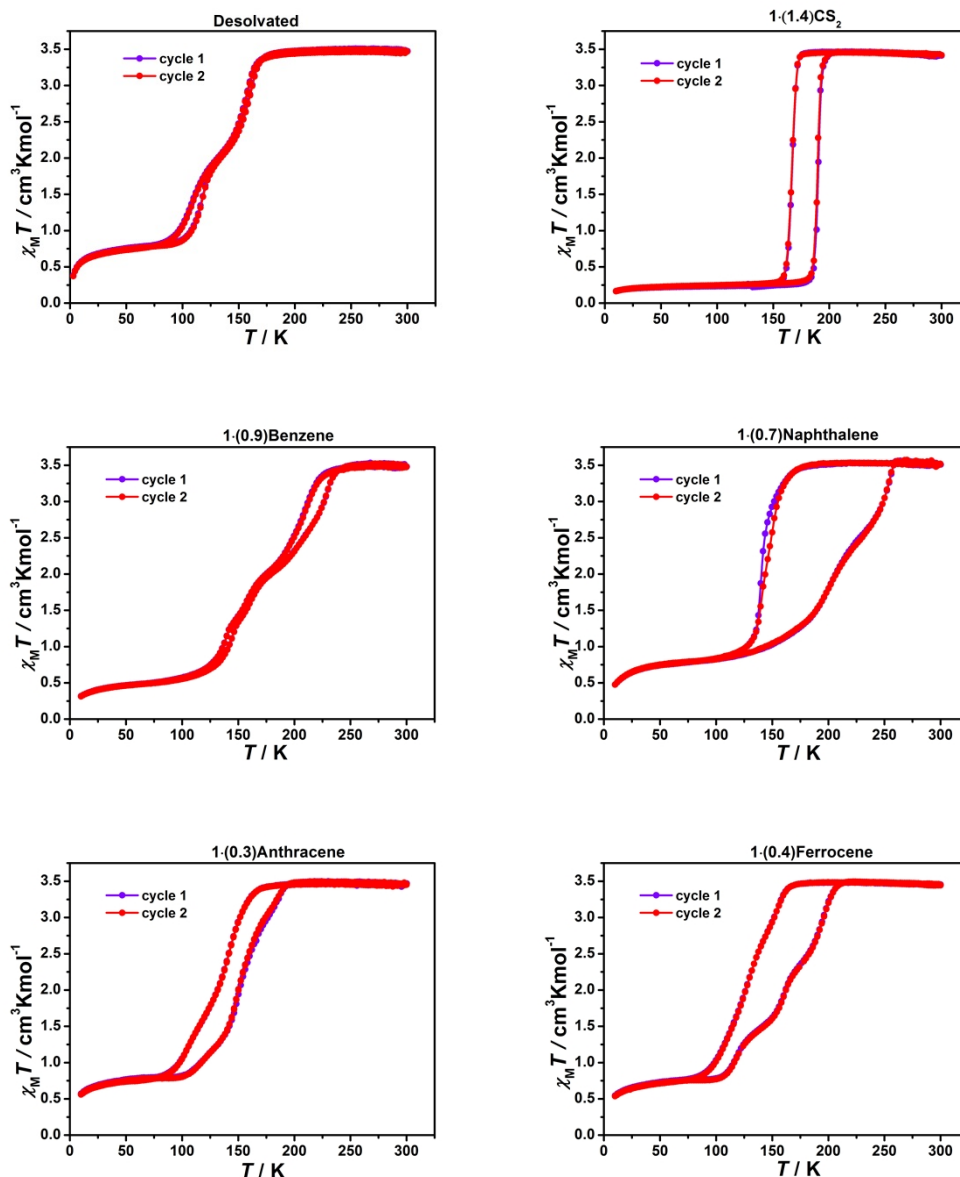


Figure S7. Variable-temperature magnetic measurements of two sequential cycles for different complexes.

Computational Details

The preferential, i.e., lowest energy, sites for guests were firstly searched by the grand canonical Monte Carlo (GCMC) simulations through the Locate task with Metropolis method based on the universal forcefield (UFF). The Mulliken charges and ESP chargers were employed to the atoms of the framework and guests molecules, respectively. During the simulations, both the framework and the individual guest molecules were regarded as rigid models. The cutoff radius was chosen as 15.5 Å for the Lennard-Jones (LJ) potential, and the maximum loading steps were 1×10^6 followed with 1×10^6 production steps, automated temperature control in the annealing cycles and 15 temperature cycles were adopted. Then the more accurate host-guest positions were further optimized by the spin-polarization periodic density function theory (PDFT) using Dmol³ codes. The widely used Perdew–Burke–Ernzerhof (PBE) function of generalized gradient approximation

(GGA) and the double numerical plus d-functions (DND) basis set combined with the DFT Semi-core Pseudopotentials (DSPP) were used. All the calculations were performed by the MS modeling 5.0 package.